Inorg. Chem. **2007**, *46*, 1502−1506

Syntheses and X-ray Diffraction, Photochemical, and Optical Characterization of $Cu_2Si_xSn_{1-x}S_3$ ($0.4 \leq x \leq 0.6$) for Photovoltaic Applications

A. Lafond,*,† J. A. Cody,‡ M. Souilah,† C. Guillot-Deudon,† R. Kiebach,§ and W. Bensch§

Institut des Matériaux Jean Rouxel, UMR 6502 CNRS-Université de Nantes, 2 rue de la Houssinière, BP 32229, 44322 Nantes, Cedex 03, France, Chemistry Department, Lake Forest College, 555 North Sheridan Road, Lake Forest, Illinois 60045, and Institut für Anorganische Chemie, Universität Kiel, Olshausenstrasse 40, 24098 Kiel, Germany

Received November 6, 2006

The study of the pseudobinary system Cu_2SnS_3–Cu_2SiS_3 shows that a solid solution ($Cu_2Si_xSn_{1-x}S_3$) exists in the range $0.4 \leq Si/(Sn+Si) \leq 0.6$. Based on diffuse reflectance and photoelectrochemical measurements these compounds show potential as absorber materials for photovoltaic devices. The compounds were prepared at 850 °C from copper sulfide, silicon, tin, and sulfur and were analyzed with single-crystal (for $x \approx 0.40$) and powder diffraction techniques. Optical band gaps of 1.25, 1.35, and 1.45 eV were observed for the three compositions $x = 0.39$, 0.48, and 0.61; cathodic photocurrent occurring is significant.

Introduction

Although the current global photovoltaic market is dominated by silicon-based technologies, thin-film chalcogenide technology could provide a real cost breakthrough to make this source of energy more competitive.[1−3] The structural, electrical, and optical properties of Cu(In,Ga)Se_2 (CIGS) make it a promising material for thin film photovoltaic devices. A few companies have developed large-scale production of modules based on the CIGS materials. Unfortunately, indium is a rare and expensive element, so it is important to seek indium-free compounds with useful photoelectronic properties.

Ab initio calculations[4] have shown that the presence of tetrahedrally coordinated copper atoms is an important feature for the good photovoltaic properties of chalcogenide absorbers. In addition, the selected compounds must have structures that can accommodate crystal defects while maintaining good electronic properties.

Among the several different related structure types of transition-metal chalcogenides, we focus our attention on the Cu_2MQ_3 series (M = Si, Ge or Sn; Q = S or Se).[5−10] Despite different crystal systems and space groups, the structure of Cu_2MQ_3 (alternative formula $Cu(Cu_{1/3}M_{2/3})Q_2$) is similar to that of $CuInSe_2$ where the In^{3+} is formally replaced by 1/3 Cu^+ + 2/3 M^{4+}.

The Cu_2MQ_3 chalcogenides are semiconductor materials with band gaps ranging from 0.84 eV for Cu_2SnSe_3[11] up to 2.5 eV for Cu_2SiS_3.[6,12] Because the band gap depends on the nature of the tetravalent metal, it is possible to obtain the optimal value[1] (1.2−1.5 eV) by a partial substitution of Si for Sn in $Cu_2(Sn,Si)Q_3$ compounds. The present paper reports the synthesis of some compounds belonging to the

* Corresponding author. E-mail: Alain.Lafond@cnrs-imn.fr.
† UMR 6502 CNRS-Université de Nantes.
‡ Lake Forest College.
§ Universität Kiel.

(1) Goetzberger, A.; Hebling, C.; Schock, H.-W. *Mater. Sci. Eng., R.* **2003**, *R40*, 1−46.
(2) Barnham, K. W. J.; Mazzer M.; Clive, B. *Nat. Mater.* **2006**, *5*, 161−164.
(3) Green, M. A.; Emery, K.; King, D. L.; Igari, S.; Warta, W. *Prog. Photovolt: Res. Appl.* **2003**, *11*, 39−46.
(4) Domain, C.; Laribi, S.; Taunier, S.; Guillemoles, J.-F. *J. Phys. Chem. Solids* **2003**, *64*, 1657−1663.
(5) Rivet, J. *Ann. Chim. (Paris)* **1965**, *1965*, 243−270.
(6) Chen, X.-A.; Wada, H.; Sato, A.; Nozaki, H. *J. Alloys Compd.* **1999**, *290*, 91−96.
(7) de Chalbaud, L. M.; Diaz de Delgado, G.; Delgado, J. M.; Mora, A. E.; Sagredo, V. *Mater. Res. Bull.* **1997**, *32*, 1371−1376.
(8) Palatnik, L. S.; Komnik, Y. F.; Belova, E. K.; Adroschenko, L. V. *C. R. Acad. Sci. (Paris)* **1963**, *257*, 161−164.
(9) Parthe, E.; Garin, J. *Monatsh. Chem.* **1971**, *102*, 1197−1208.
(10) Delgado, G. E.; Mora, A. J.; Marcano, G.; Rincon, C. *Mater. Res. Bull.* **2003**, *38*, 1949−1955.
(11) Marcano, G.; Rincon, C.; de Chalbaud, L. M.; Baracho, D. B.; Sanchez Perez, G. *J. Appl. Phys.* **2001**, *90*, 1847−1853.
(12) Aruga, A.; Okamoto, Y. *Jpn. J. Appl. Phys.* **2006**, *45*, 4616−4620.

10.1021/ic0621087 CCC: $37.00
Published on Web 01/24/2007

Cu_2SnS_3−Cu_2SiS_3 system, the crystal structure determination of one of these phases ($Cu_2Sn_{0.63}Si_{0.37}S_3$), and the study of the solid solution. In addition we present the preliminary investigations of the diffuse reflectance and photoelectrochemical properties.

Experimental Section

Synthesis. The compounds $Cu_2Si_xSn_{1-x}S_3$ were prepared by the solid-state reaction of Cu_2S, Sn, Si, and S in the appropriate ratios to get the compositions $x = 0.40$, 0.50, and 0.60. The reactants were ground together and pressed into a pellet before being heated in evacuated, sealed, fused silica tubes. The synthesis route was adapted from Chen et al.[6] and from Olekseyuk et al.[13] The tubes were heated slowly to 850 °C, held there for 1 week, cooled to 650 °C, held there for several hours, and then quenched in water. The samples were carefully reground and reheated at 650 °C for 2 weeks and quenched in water again. Usually, a third heating at the same temperature for 1 week is necessary to obtain a homogeneous powder. On the other hand, single crystals were obtained from powder with composition close to $x = 0.4$ by adding iodine as a transport agent during a subsequent heating step.

EDX. The chemical compositions of the samples were analyzed using an EDX-equipped scanning electron microscope (JEOL 5800LV). These analyses were performed on polished sections of the products imbedded in epoxy. The elemental percentages were calculated using calibrated internal standards; the uncertainty of EDX spectra curve fitting is similar in magnitude to the standard deviations for the averages. Thus, the results are both accurate and precise.

X-ray Diffraction. A single-crystal structure determination was performed for one composition ($x \approx 0.4$). The data collection was carried out on a Bruker-Nonius Kappa CCD diffractometer using graphite monochromated Mo Kα. Many crystals were examined to find one of suitable quality. Crystals were mounted on the tip of broken capillary tubes. Although a monoclinic symmetry was expected,[14] we recorded the full diffraction sphere to ensure high redundancy and thus to obtain well-measured intensities. Cell parameters of the best crystal were indeed consistent with monoclinic symmetry. Technical details of data collection are given in Table 1.

Homogeneity of powder samples was evaluated by examination of the X-ray powder diffraction patterns. These experiments were performed with the use of a position-sensitive detector diffractometer (INEL) set up in a Debye−Scherrer geometry (Cu Kα1 radiation and $Na_2Ca_3Al_2F_{14}$ as standard[15]). The powder patterns were recorded in the range 0−120° 2θ with 0.03° 2θ-steps. The samples were ground and passed through a sieve before they were put into a Lindemann capillary (0.2 mm in diameter). The full pattern matching and Rietveld refinements were carried out with the help of the programs FullProf[16] and WinPlotr.[17]

Diffuse Reflectance Measurements. The UV−visible diffuse reflectance spectra of finely ground samples of different compositions were recorded with a Varian CARY 5G spectrometer equipped with a praying mantis mirror configuration and controlled using the CARY WinUV program. The reflectance measurements were made in the 1200−600 nm range (i.e., from 1.03 to 2.07 eV) at 2 nm resolution. The measured reflectance was normalized to a barium carbonate blank. The absorption (K/S) data were calculated from the reflectance spectra using the $K/S = (1-R)^2/2R$ Kubelka−Munk function.[18,19]

Photoelectrochemical Measurements. The electrochemical measurements were performed with a simplified three-electrode setup. The sintered and pressed powder samples were embedded in an epoxy resin with a silver back contact; the front faces were polished to a high shine. A small amount of aqueous electrolyte (H_2SO_4 solution, pH ≈ 1) was deposited on the polished surface (∼10 mm^2). A platinum electrode was put into the solution and was connected to both the counter electrode and the reference outputs of the potentiostat. The sample was illuminated with a 150 W white lamp providing an illumination intensity of approximately 30 W/cm^2. During the cyclic voltammetry measurements the light was manually chopped to highlight the photoresponse.

Table 1. Experimental Details for Single-Crystal Data Collection for $Cu_2Sn_{0.63}Si_{0.37}S_3$

crystal data	
chemical formula	$Cu_2Sn_{0.63}Si_{0.37}S_3$
molar mass (g/mol)	308.45
cell setting, space group	monoclinic, *Cc* (no. 9)
a, *b*, *c* (Å); ss (deg)	6.542(2), 11.413(5), 6.532(2); 108.79
V (Å^3); *Z*	461.73; 4
Dx (g.cm^{-3}); μ (mm^{-1})	4.436; 13.833
crystal size mm	0.131 × 0.084 × 0.076
data collection	
radiation type	Mo *K*α
absorption correction	Gaussian method
*T*min, *T*max	0.2814, 0.4552
no. of measured reflcns	9646
no. of independent reflcns	2426
no. of observed reflcns (I > 2σ(I))	1946
θ_{range} (deg)	6.59−40.00
range of *h*, *k*, *l*	$-11 \le h \le 10$, $0 \le k \le 20$, $-11 \le l \le 11$
R_{int}	0.0446
refinement	
R, R_w, S (g o.f)	0.0404 0.0479, 1.29
no. of parameters	55
weighting scheme	$w = 1/[\sigma^2(F) + 0.0004F^2]$
ρ_{max}, ρ_{min} (e.Å^{-3})	0.95, −0.87
extinction method	isotropic type I
extinction coefficient	0.062

Table 2. Atomic Positions and Equivalent Displacement Parameters for Synthetic $Cu_2Sn_{0.63}Si_{0.37}S_3$

atom	*x*	*y*	*z*	U_{eq}	sof[a]
Cu1	−0.0283(2)	0.41426(5)	−0.02040(19)	0.0257 (4)	1
Cu2	−0.0161(2)	0.25030(5)	0.47835(19)	0.0256(3)	1
Sn1/Si1	0[b]	0.08872(3)	0[b]	0.01207(9)	0.627(2)/0.373(2)
S1	0.3662(3)	0.08416(9)	0.1073(2)	0.0206(3)	1
S2	0.3568(3)	0.25214(10)	0.6083(3)	0.0210(3)	1
S3	0.3574(2)	0.41847(9)	0.1154(3)	0.0209(3)	1

[a] sof: site occupancy factor. [b] These values were fixed to 0 to define the origin of the unit cell.

(13) Olekseyuk, I. D.; Piskach, L. V.; Zhbankov, O. Y.; Parasyuk, O.; Kogut, Y. *M. J. Alloys Compd.* **2005**, *399*, 149−154.
(14) Onoda, M.; Chen, X.-A.; Sato, A.; Wada, H. *Mater. Res. Bull.* **2000**, *35*, 1563−1570.
(15) Deniard, P.; Evain, M.; Barbet, J. M.; Brec, R. *Mater. Sci. Forum* **1991**, *363*−*82*, 79.
(16) Rodríguez-Carvajal, J. *Physica B* **1993**, *192*, 55−69.
(17) Roisnel, T.; Rodriguez-Carvajal, J. *Mater. Sci. Forum* **2001**, *378*−*381*, 118−123
(18) Kubelka, P. *J. Opt. Soc. Am.* **1948**, *38*, 448−457.
(19) Kubelka, P.; Munck, F. *Z. Tech. Phys.* **1931**, *12*, 593−601.

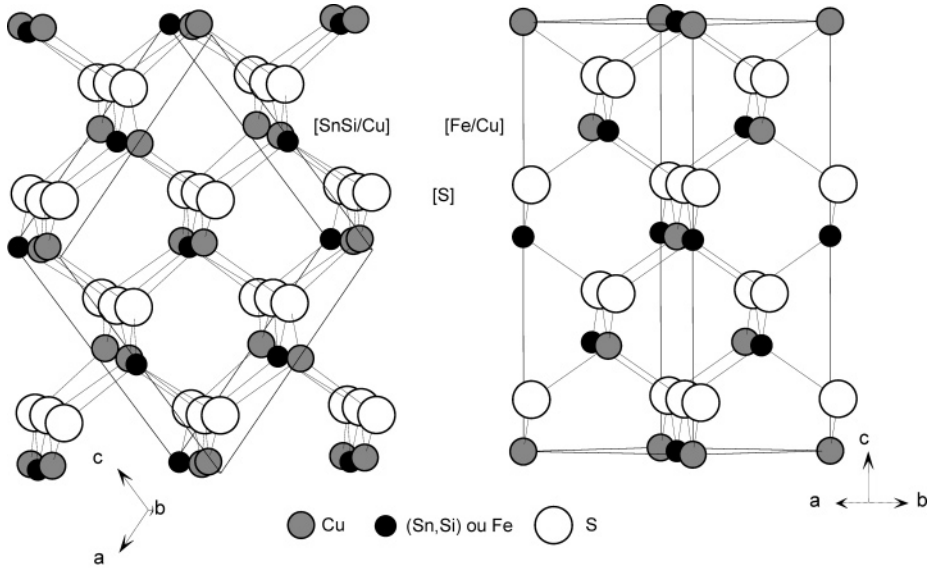

Figure 1. Projection of the structures of (a) $Cu_2Si_{0.37}Sn_{0.63}S_3$ (S.G. *Cc*) from the single-crystal structure solution presented here and (b) $CuFeS_2$ (S.G. *I*-42*d*).[27]

Single-Crystal Structure Determination

Structure Refinement. The crystal for the structure determination was selected from a preparation with $x = 0.4$. The set of the recorded reflections is consistent with the space groups *C*2/*c* and *Cc*. The centrosymmetric space group *C*2/*c* was examined and then rejected. Starting from the Cu_2SnS_3 structure,[14] the crystal structure was refined in the space group *Cc* using the Jana2000 program.[20] The crystal shape and size optimizations for absorption corrections were performed using the program X-shape.[21] Crystal characteristics and refinement results are gathered in Table 1. With anisotropic atomic displacement parameters for all atoms and fixing Sn and Si atoms on the same site, the residual value converged to $R = 0.0404$ ($R_w = 0.0479$) for 1946 reflections satisfying the criterion $I > 2\sigma(I)$ and 55 parameters. Since the *Cc* space group is noncentrosymmetric, we checked the correctness of the configuration by calculating the amount of the other enantiomorph present as a twin; this value converged to 0.04(2). Then, the proposed absolute structure is definitively correct in agreement with the parent compounds Cu_2SiS_3 and Cu_2SnS_3. The chemical composition deduced from the last stage of the refinement was $Cu_2Sn_{0.63}Si_{0.37}S_3$. The atomic coordinates are given in Table 2.

Description of the Crystal Structure. Cu_2SnS_3, $Cu_2Sn_{0.63}Si_{0.37}S_{30}$, and Cu_2SiS_3 all adopt the same monoclinic structure that can be derived from the chalcopyrite type ($CuFeS_2$) with tetragonal symmetry and space group *I*-42*d* (Figure 1). The relationship between the two structures is consistent with their noncentrosymmetric character. In $CuFeS_2$, the Cu and Fe atoms are located on two different sites with similar tetrahedral coordination of S atoms. Compounds of the type Cu_2MS_3 (M = Sn, Si or (Sn,Si)) can be reformulated as $Cu(1)(Cu(2)_{1/3}M_{2/3})S_2$, where the Fe^{3+} is replaced by 1/3 $Cu(2)^+$ + 2/3 M^{4+}, thus retaining charge balance. This situation is consistent with the observed lowering of symmetry so that the Cu(2) and M atoms become nonequivalent and the Sn and Si atoms are statistically distributed over the same crystallographic site. The difference of the ionic radii of Sn^{4+} and Si^{4+} leads to a distortion of the structure. Consequently, all cations are found in distorted tetrahedral coordination with Cu−S and (Sn,Si)−S distances in ranges 2.30−2.39 Å and 2.26−2.38 Å, respectively. The calculation of bond valences according to Brown[22] suggest the presence of Cu(I) and yield an average value of 4.0 for the mixed site Sn/Si ($0.63 \times 4.97 + 0.37 \times 2.40 = 4.0$) in good agreement with Sn(IV) and Si(IV).

Table 3. Results of EDX Analysis on Polished Sections of Powder Samples for $Cu_2Si_xSn_{1-x}S_3$ ($x = 0.4, 0.5, 0.6$)[a]

	average atomic %				
sample (no. of spots)	Cu	Sn	Si	S	*x*
0.40 (expected)	33.3	10.0	6.7	50.0	
# 1 (3)	31.8(8)	10.6(2)	6.9(3)	50.8(7)	0.39
# 2 (9)	33.3(9)	10.3(3)	6.5(2)	49.9(6)	0.39
0.50 (expected)	33.3	8.3	8.3	50.0	
# 3 (12)	32.7(5)	8.9(3)	8.1(4)	50.4(6)	0.48
# 4 (11)	33.8(6)	8.6(9)	7.9(7)	49.8(6)	0.48
0.60 (expected)	33.3	6.7	10.0	50.0	
# 5 (4)	32.8(1.8)	7.4(6)	10.7(1.0)	49(2)	0.59
# 6 (10)	33.0(8)	6.6(4)	10.4(2)	50.0(6)	0.61

[a] The ESD given in parentheses correspond to the dispersion of the averaged values. The *x* values (last column) are calculated as atom %(Si)/(atom %(Si)+atom %(Sn)).

Existence of the Solid Solution

Results of careful EDX analyses on several samples of nominal compositions $x = 0.4$, 0.5, and 0.6 are presented in Table 3. The average measured compositions are close to the ratios expected from the starting material stoichiometry. In addition, the individual compositions of these samples are

(20) Petricek, V.; Dusek, M. *Jana2000 Structure Determination Software Programs*, 2000.
(21) Stoe&Cie, *X-Shape*; 1996.
(22) Brown, I. D.; Altermatt, D. *Acta Crystallogr.* **1985**, *B41*, 244−247.

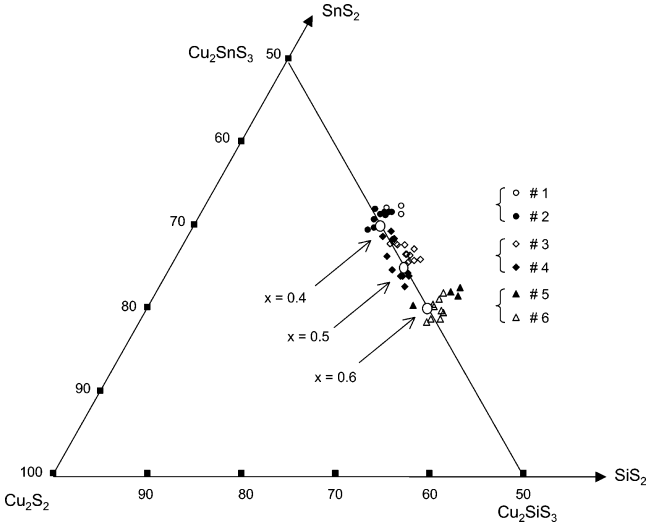

Figure 2. Atomic compositions according to EDX measurements of individual spots for several samples of $Cu_2Si_xSn_{1-x}S_3$ on the pseudoternary diagram. The open circles correspond to the target compositions of x = 0.4, 0.5, and 0.6.

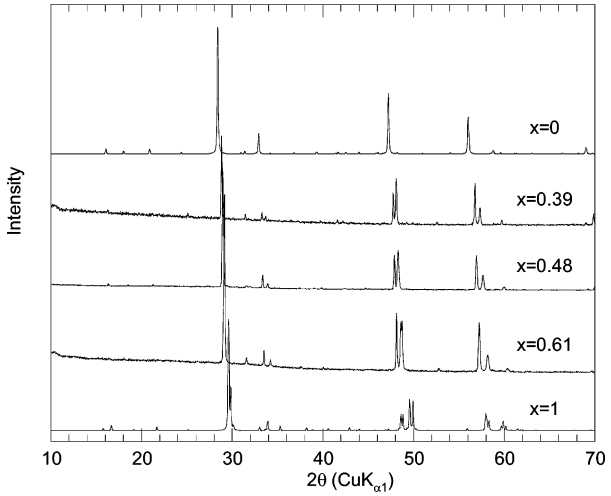

Figure 3. Comparison of experimental XRD patterns for synthesized compounds and calculated patterns for Cu_2SnS_3 ($x = 0$[14]) and Cu_2SiS_3 ($x = 1$[6]). The actual compositions are given by EDX results.

plotted on a pseudoternary diagram (Figure 2). Because these compositions are located on the $Cu_2SnS_3-Cu_2SiS_3$ line (atom %(Cu) and atom %(S) are constant) one can conclude that the substitution of Si for Sn could occur in these compounds resulting in a solid solution in the $Cu_2SnS_3-Cu_2SiS_3$ system that is consistent with the structural investigation described above.

The existence of a solid solution can be confirmed with the help of powder X-ray diffraction analyses. The XRD patterns for the targeted compositions $x = 0.4$, 0.5, 0.6 and for the pure ternary compounds Cu_2SnS_3 ($x = 0$) and Cu_2SiS_3 ($x = 1$) are sufficiently similar (see Figure 3) to indicate that all are isostructural. The evolution of the peak positions is consistent with the relative values of the ionic radii of Si^{4+}(0.40 Å) and Sn^{4+}(0.69 Å).[23] Unit cell parameters were refined from the XRD patterns by the Le Bail method[24] and

(23) Shannon, R. D. *Acta Crystallogr.* **1976**, *A32*, 751−767.
(24) Le Bail, A.; Duroy, H.; Fourquet, J. L. *Mater. Res. Bull.* **1988**, *23*, 447−452.

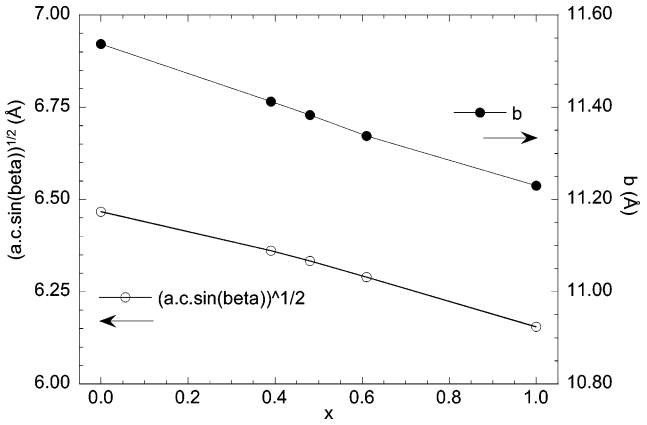

Figure 4. Evolution of the cell parameters (see Table 4) versus the actual compositions of $Cu_2Si_xSn_{1-x}S_3$. The values for $x = 0$[14] and $x = 1$[6] come from the published single-crystal structure determinations.

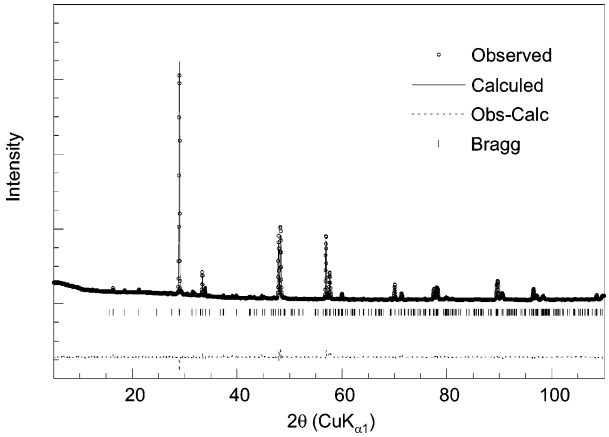

Figure 5. Rietveld refinement results for the sample #3 ($x = 0.48$). Final agreement factors are $R_p = 3.6$, $R_{wp} = 5.2$, $R_B = 9.2$, and $\chi^2 = 5.7$.

Table 4. Unit Cells Parameters Determined from X-ray Powder Diffraction[a]

x	0	0.39	0.48	0.61	1
a (Å)	6.653(1)	6.5390(2)	6.4960(4)	6.4428(4)	6.332(1)
b (Å)	11.537(2)	11.4127(6)	11.3835(9)	11.3382(7)	11.23(1)
c (Å)	6.665(1)	6.5367(6)	6.5152(4)	6.4687(4)	6.273(1)
β (°)	109.39(3)	108.787(4)	108.612(6)	108.368(5)	107.49(1)
V (Å^3)	482.56	461.83	456.59	448.46	425.4(1)

[a] The values for $x = 0$[14] and $x = 1$[6] come from the published single-crystal structure determinations.

are given in Table 4. Because the monoclinic angle decreases slightly when x increases, Figure 4 shows the variation of $(a\times c\times \sin\beta)^{1/2}$ and b versus the silicon content for several samples of $Cu_2Si_xSn_{1-x}S_3$.

In addition, the homogeneity of a powder sample with composition $x = 0.48$ was examined through a full Rietveld analysis of the X-ray pattern. The refinement was done starting with the single-crystal structural model. Figure 5 gives the calculated and the experimental patterns.

Optical Properties Investigations

Figure 6 shows the reflectance spectra of several compounds with actual compositions of $x = 0.39$, $x = 0.48$, and $x = 0.61$. The band gaps were determined as the intersection point between the energy axis and the line extrapolated from

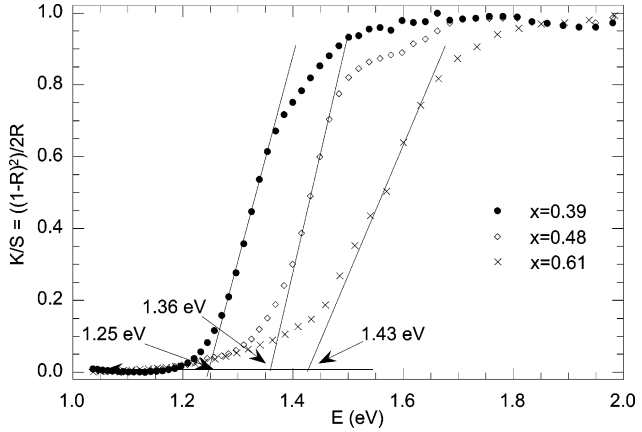

Figure 6. Absorption spectra (K/S) for different samples of $Cu_2Sn_{1-x}Si_xS_3$ after the Kubelka−Munk transformation $K/S = (1-R)^2/2R$. To facilitate comparison, the spectra have been normalized.

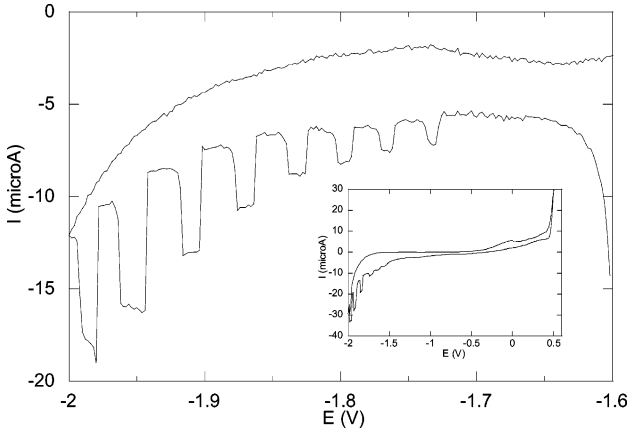

Figure 7. Cyclic voltammograms of $Cu_2Sn_{0.5}Si_{0.5}S_3$ recorded under UV illumination. Manual chopping of the signal can be observed in the −2 to −1.5 eV range in both the full curve and inset.

the linear portion of the absorption edge in the K/S vs E plots. The obtained values are approximately 1.25, 1.35, and 1.45 eV for $x = 0.39$, 0.48, and 0.61, respectively. Obviously, from these data the accuracy of the determined band gap is not very high; nevertheless, the clear trend is that the band gap increases when Sn is replaced by Si. The evolution of the band gap within the $Cu_2Si_xSn_{1-x}S_3$ solid solution is consistent with the data observed for the parent compounds Cu_2SnS_3 ($E_g = 0.9$ eV)and Cu_2SiS_3 ($E_g = 2.5$ eV). A similar trend was found in the copper-chalcopyrite series $CuMS_2$: $E_g(CuInS_2) = 1.53$ eV, $E_g(CuGaS_2) = 2.43$ eV, and $E_g(CuAlS_2) = 3.49$ eV.[25]

Since the observed band gap is in the desired range for solar cell materials, the photocurrent must be measured to determine the potential interest of the material for possible device construction. Preliminary examination of the material through photoelectrochemical measurements shows an observable, cathodic photocurrent. The dramatic result of manual chopping of high-energy light on the reduction part of the I−V curve is clearly seen in Figure 7.

Discussion and Concluding Remarks

The study of the Cu_2SnS_3−Cu_2SiS_3 pseudobinary system demonstrates that the structure of compounds with compositions $Cu_2Si_xSn_{1-x}S_3$ is derived from the chalcopyrite type $CuFeS_2$. From a charge balancing point of view 1 Fe^{3+} is replaced by 1/3 Cu^+ + 2/3 M^{4+} with M = Sn,Si. In the present work the existence of the solid solution $Cu_2Sn_{1-x}Si_xS_3$ was highlighted between $x = 0.4$ and 0.6. But we can expect that this solid solution is continuous from $x = 0$ to $x = 1$. The crystal structure determination and the X-ray powder diffraction studies corroborate this hypothesis. Indeed the compounds crystallize in a monoclinic structure like the pure phases, and there is a smooth decrease in the crystallographic parameters with x despite the large difference between the radii of Sn and Si. The results of the present study show that the Cu_2MS_3 structure type is sufficiently adaptable to accommodate chemical substitutions of tetravalent cations. The preliminary investigations of the optical properties are promising. The change of the band gap across the substitution series clearly indicates that it is possible to adjust the gap to the optimal value (1.2−1.5 eV) for solar light absorption. According to the photoelectrochemical investigation, the photoinduced currents in the bulk samples are cathodic, indicating that they are p-type semiconductors[26] just like CIGS compounds. In addition, the magnitude of the photocurrent for $Cu_2Sn_{1-x}Si_xS_3$ compounds is quite high compared to the dark current. Both results suggest that these compounds are good candidates for photovoltaic applications. Further studies of this class of compounds are under way including the study of the structural stability with respect to variations of the copper stoichiometry and electrical conductivity measurements on bulk samples.

Acknowledgment. J.A.C. gratefully acknowledges Lake Forest College and the University of Nantes for his research sabbatical. R.K. acknowledges the State of Schleswig-Holstein to have supported his stay at IMN. The authors thank J.-F. Guillemoles (IRDEP) for his help with the photoelectrochemical measurements.

Supporting Information Available: Crystallographic data for $Cu_2Si_{0.37}Sn_{0.67}S_3$ in CIF format. This material is available free of charge via the Internet at http://pubs.acs.org.

IC0621087

(25) Jaffe, J. E.; Zunger, A. *Phys. Rev. B* **1983**, *27*, 5176−5179.

(26) Honda, K. *J. Photochem. Photobiol., A* **2004**, *166*, 63−68.

(27) Pauling, L.; Brockway, L. O. *Z. Kristallogr.* **1932**, *82*, 188−194.